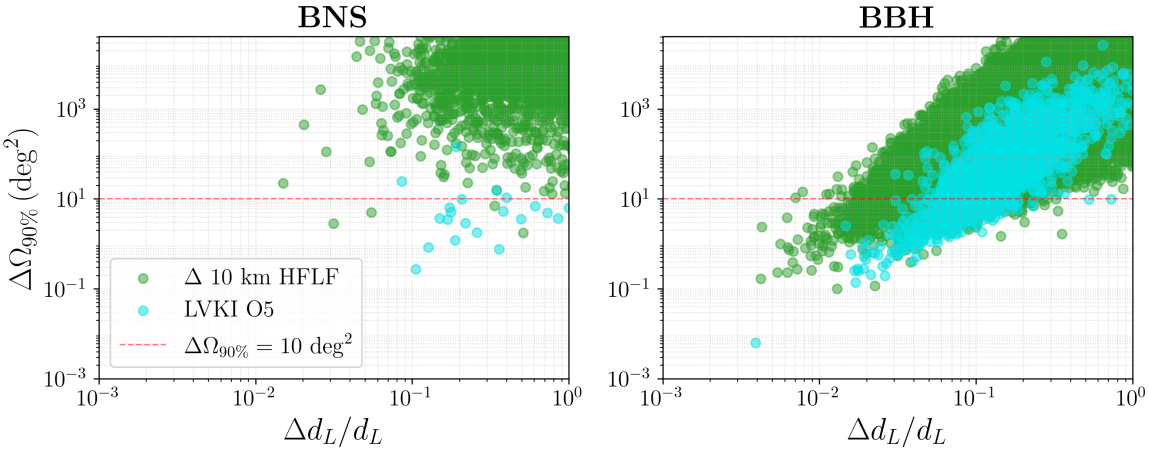

Figure 80. The joint accuracy on luminosity distance ($\Delta d_L/d_L$) and angular resolution ($\Delta\Omega_{90\%}$) for BNS (left) and BBH (right). Green shows results from the triangular ET detector (10-km arms) with both high- and low-frequency instruments (HFLF). Light blue indicates forecasts for LVKI O5, the most advanced 2G detector network (LIGO Hanford, LIGO Livingston, Virgo, KAGRA, and LIGO India) [392]. The dashed red line represents a 10 deg^2 sky localization error. Reproducedfrom [16]. The Author(s). CC BY 4.0.

detail in section 3.3.1, provides an alternative measurement of current methods to constrain the cosmological parameters such as the Hubble constant. Second, galaxy formation and evolution throughout the history of the Universe affects stellar populations, thereby shaping the likely pathways for compact object mergers (section 4.9.2). Here, we explore these aspects in anticipation of future detections with ET.

4.9.1 Multi-messenger detections and sky localization of the host galaxies

The large sky localization inferred with current GW detectors, spanning hundreds of square degrees [392], represents a challenge for host galaxy identification. The impact of this uncertainty on the efficiency of host galaxy identification is substantial, as it determines the number of pointings required by electromagnetic instruments to cover the GW signal location and the corresponding observational time to be used. This challenge, however, holds promising prospects with the deployment of ET. Its low-frequency sensitivity promises to observe binary compact objects for a longer period of time before the merger occurs [16]. For instance, a BNS signal analogous to GW170817 can be visible by ET $>$ 20 hours before merger [1167] (see also figure 198 in section 11). This aspect will significantly increase the number of BHNS and BNS mergers with a sky localization of less than 10 square degrees [16, 1167, 2182]. Figure 80 shows that the angular resolution expected for the most advanced 2G network at full O5 sensitivity (LVKI O5: LIGO Hanford, LIGO Livingston, Virgo, KAGRA, and LIGO India) is similar to that of a single 10-km ET triangular observatory. However, ET detects over 10 times more events, including those with high SNR, resulting in a nearly tenfold reduction in the error on luminosity distance [16].

Despite the improved sky localization achieved with ET, the electromagnetic follow-up process still tipically entails scanning through multiple galaxies (although in some case

JCAP03(2026)081

the angular resolution could be sufficiently good that there will be only one galaxy in the localization volume, see figure 47 in section 3). Therefore, optimized follow-up strategies can be accomplished through simulation-informed ranking of galaxies within a given sky localization. We can derive the probability that a galaxy hosts a compact object coalescence based on various properties, such as its stellar mass and star formation rate (see e.g. [2183–2186]. The refinement of simulation-informed ranking, where multiple formation scenarios of compact object mergers are taken into account, is particularly crucial for identifying the host galaxies of compact objects where electromagnetic emission is impossible or improbable, such as BBH mergers and BHNS mergers [2187].

As we saw in section 3.3.1, host galaxy identification is also crucial in the use of compact binary mergers as "bright" sirens, in order to infer cosmological parameters. As discussed in particular in section 3.3.1.2, even with the lack of an EM counterpart detection, galaxies with known redshift within the sky localization can be ranked and used to infer the cosmological parameters with statistical methods, particularly if the localization volume contains a limited number of possible host galaxies. The thousands of GW events that ET will detect with its improved sky localization will provide a significant step forward in determining cosmological parameters.

4.9.2 Formation channels and their link with galaxy properties

As we have discussed, the improvements expected for third-generation detectors will provide a number of simultaneous identification of GW events and their host galaxies at different cosmic times [16], either through the detection of an electromagnetic counterpart (at least for BNSs) or, for BBHs, through the statistical association with a limited number, or possibly just a single host galaxy in the localization volume. These concurrent detections (or statistical associations) offer a unique opportunity to gain additional insights into the underlying physics governing the formation channels and evolution of compact objects (see e.g. [2188–2195]).

As mentioned previously (see section 4.1 and reference therein), the two main proposed pathways are the isolated formation channel, which includes processes like common envelope evolution, chemically homogeneous evolution, and stable mass transfer; and the dynamical formation channel taking place in dense stellar clusters (e.g. galactic center, open star clusters, globular clusters and young star clusters). Current detections suggest that multiple formation channels are needed to explain the origin of BBHs (see e.g. [1570]). Furthermore, most binary compact object systems are formed in galaxies. Therefore, the host galaxy properties are an excellent complement to understand the role of the different formation channels of gravitational-wave events across cosmic time.

Galaxy formation and evolution is regulated by a large diversity of baryonic processes shaping their star formation history, chemical enrichment, stellar mass, gas abundance, among others [2196]. These factors impact the stellar populations' properties and, in turn, the most favorable formation channels of binary compact object mergers.

For instance, galaxies in high-dense regions often undergo major mergers increasing the probability of hosting a large number of stellar clusters [2197, 2198]. These galaxies, in turn, would produce more BBHs through dynamical interactions [1630]. Notably, observations from the local Universe indicate a strong dependence of the number and mass of globular

JCAP03(2026)081

clusters on the total stellar mass of the galaxies, and a tendency to be more numerous in early-type galaxies [2199–2201]. Furthermore, stellar clusters and active galactic nuclei are considered potential factories of BBH mergers in the pair-instability mass gap and above (see e.g. [1498, 1541, 1630]).

The delay time, defined as the time for compact objects to merge, is important for connecting galaxy properties with binary compact object formation channels. It depends on the outcome of specific physical processes experienced by stars in binary systems such as the common envelope phase in the isolated scenario (see section 4.1). In particular, the number of mergers that occur in massive and passive galaxies tends to increase when the delay time is longer [2184, 2202]. The wide redshift range expected for ET detections [10, 12, 15], together with their electromagnetic counterparts will play a fundamental role in deciphering the contribution of the different formation channels across cosmic time.

The chemical abundance of the stellar populations within galaxies is another key piece of information. Theoretical inferences from binary population synthesis simulations suggest the efficient formation of BBHs at sub-solar metallicities [1198, 1371, 1597, 1603, 2203]. Consequently, low-mass galaxies ($< 10^8 M_\odot$) emerge as promising sites for detecting these mergers [1249, 1606]. However, their faintness and high-redshift nature ($z > 4$) make them challenging to constrain through EM observations. As a result, ET emerges as a promising tool for delving into the chemical evolution of galaxies [1617, 2204]. As host galaxies leave distinctive imprints on compact object mergers throughout cosmic time, the identification capability of ET becomes crucial. If these galaxies have features like low mass and low metallicity, it implies a relatively short delay time for BBHs on average. This breakthrough will effectively resolve the degeneracy between the impacts of formation metallicity and delay time distribution [1604], addressing a significant challenge in gravitational-wave astrophysics. This is also shown in figure 81 schematically.

4.10 Populations backgrounds

The incoherent superposition of the GW signal from all astrophysical sources in our Universe creates a stochastic background whose amplitude and spectral shape reflect the properties of each source population contributing to it. The stochastic GW background (SGWB) is thus a powerful astrophysical probe, complementary to the detection of individual astrophysical sources.

As discussed in section 3.1.1 a SGWB, either of astrophysical or cosmological origin, is characterised in terms of the dimensionless energy density parameter, defined in eq. (3.12), that we recall here,

$$\Omega_{\rm GW}(f) = \frac{1}{\rho_c}\frac{{\rm d}\rho_{\rm GW}(f)}{{\rm d}\ln f}\,, \tag{4.5}$$

where ρ_c is the critical energy of the Universe. The astrophysical component can be schematically parametrised as:

$$\Omega_{\rm GW}(f) = \frac{f}{\rho_c c^2}\sum_{\rm i}\int_0^{z_{\rm max}}\int_\lambda \frac{R_{\rm i}(z,\lambda)\; P_i(\lambda)}{(1+z)\,H(z)}\frac{{\rm d}E_{\rm GW,i}(f_s,\lambda)}{{\rm d}f_s}\,{\rm d}\lambda\,{\rm d}z\,, \tag{4.6}$$

JCAP03(2026)081

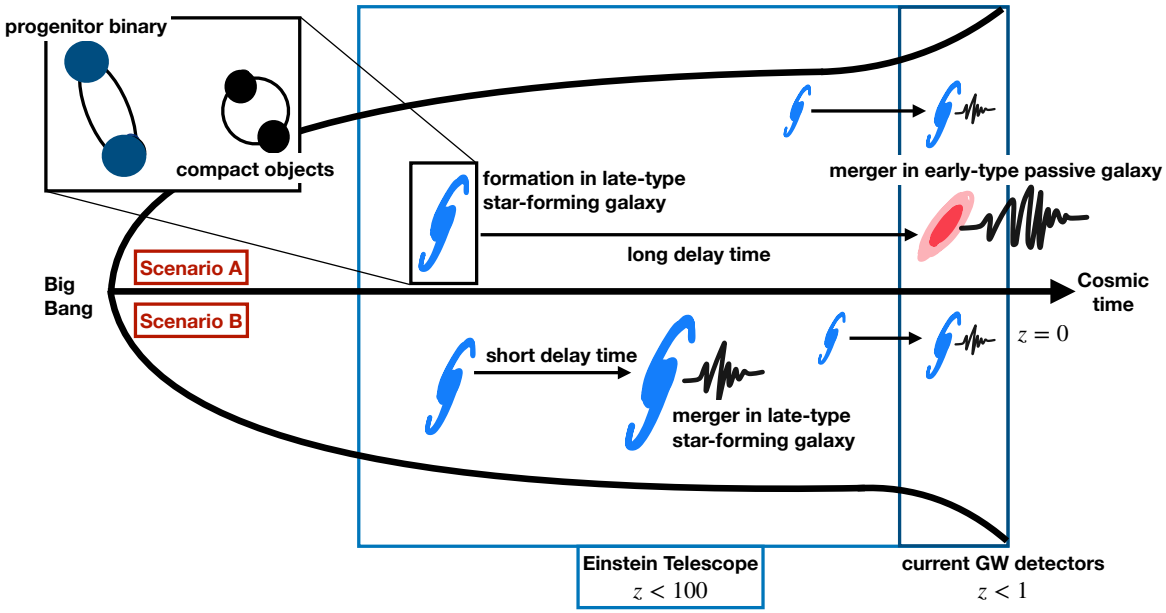

Figure 81. ET will explore the interplay between the physics of compact objects, originating from massive stars, and the galaxies hosting their mergers. Presently, with current GW detectors, exploration is confined to the local Universe ($z < 1$), where mergers can occur in early-type passive galaxies, like NGC 4993 which hosted GW170817. In contrast, ET will be able to observe BBH mergers with sky localization error of less than $10\,\mathrm{deg}^2$ up to $z \sim 6$ (see figure 10 in [16]), opening to completely new perspectives in host galaxy identification.

where $H(z)$ is the Hubble parameter, the index i runs over different source classes (such as BBH, BNS, supernovae, neutron stars) and the parameter λ encodes all the source properties of each class (such as masses and spins for CBC, ellipticity for rotating neutron stars etc.). Finally, $R_\mathrm{i}(z, \lambda)$ is the rate of each source and $\mathrm{d}E_{\mathrm{GW,i}}(f_s, \lambda)/\mathrm{d}f_s$ is the energy spectrum it emits.

We will focus our discussion here on CBCs and the unique information that can be obtained with ET. The main challenges are studying BBH formation channels, searching for Population III stars and detecting the residual BNS background. We will also mention other sources and their contribution to the SGWB and discuss synergies with electromagnetic observations.

We note that the background defined in eq. (4.6) is the total background. In the case of CBCs, it can be relevant to study the residual background obtained after subtracting individually detected sources. On the one hand this background is complementary from individual detection and can provide statistical information about the faintest sources at the largest distances, and on the other hand subtracting sources can help observing backgrounds that are masked by the total background. For LIGO-Virgo-Kagra, the number of sources detectable individually is sufficiently small so that the distinction between total background and residual one (obtained after resolvable sources are filtered out), is very mild. However, with its highly improved sensitivity, ET will detect a very large number of individual sources: their accurate subtraction is crucial and will pose itself an interesting challenge. Indeed, as

JCAP03(2026)081

discussed in section 10.5.3, suboptimal individual sources subtraction will manifest itself as an additional stochastic component. In the rest of this section we will assume that source subtraction is completely noiseless and discuss the scientific questions that SGWB observations can address. We will discuss both the total background (without subtraction) and the residual background (obtained after noiseless subtraction).

We note that, even if most of the BBHs are expected to be detectable individually by ET, this will not be the case for a population of BNSs: since they are fainter than BBH and with a longer time in band, they are expected to produce superposed signals, and the bulk of the population is expected to be subthreshold (see figure 14 of [1167] or figure 107 in section 10). A background approach will provide us with information on this population that cannot be achieved with a catalog (individual detections) approach alone. However, even for BBHs, using a background approach to reconstruct parameters such as merger rate and mass distribution is useful to perform a cross-check with the same quantities extracted from a catalog. A discrepancy might be the indication of the presence of a faint subpopulation, that is not captured when looking at individual events. A population of PBHs extends to redshift higher than the instrument horizon, and the properties of a high-z population can be extracted only with a background approach. Finally, since astrophysical backgrounds represent a foreground for sources of primordial origin, understanding their properties is crucial for accurately subtracting their contribution from an observed background map and looking at cosmological components.

4.10.1 Study of BBH formation channels

Detection and characterization of the SGWB will provide additional information on source population properties. One of the main contributions to the signal in ET is expected to be from BBH mergers occurring at relatively low redshifts ($z < 5$), with masses in the range $\sim (10 - 10^3)\, M_\odot$ [16]. The formation channels of these BBH, as discussed in section 4.1, can be broadly divided into the isolated channel (including formation from isolated field pairs and multiples), and the dynamical channel. The latter including formation in globular (GC), nuclear (NSC) or young star clusters (YSC), and gas-driven formation in AGN disks. These formation channels leave an imprint on the masses, spins and eccentricities of the resulting BBH, as well as the merger rate, the distribution of time delays and the evolution of the mass spectrum with redshift. These differences will manifest themselves in the SGWB detectable with ET.

As an example, in figure 82 we show the contributions to the SGWB from BBH formed via the isolated channel (Field) and three variants of the dynamical channel: YSC, NSC and GC. All the computations were performed with the public code `PRINCESS`[43] using population models from [338]. We show both the total and residual backgrounds, where the latter are computed by removing all sources having an individual SNR $\rho_{\text{thrs.}} > 20$ (neglecting the error in the subtraction; see section 10.5.3 for the treatment of the subtraction error) and assuming a random inclination and position in the sky. The shaded areas shown for the Field, YSC and GC channels reflect the uncertainty in the merger rates for each population model, and are derived from table 2 in [338]. The model uncertainty of the NSC channel is relatively small

[43] See https://gitlab.com/Cperigois/Princess.

JCAP03(2026)081

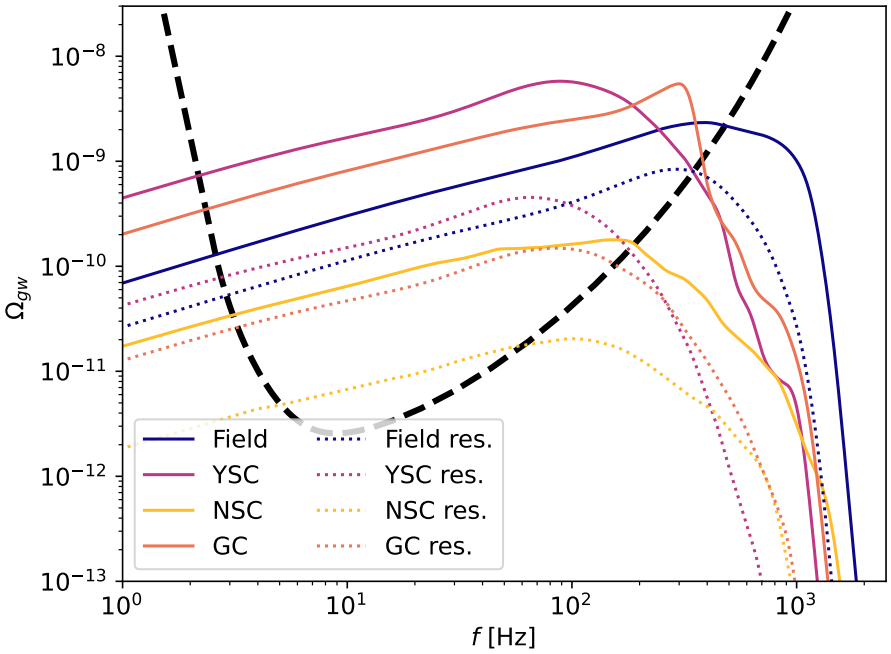

Figure 82. Background energy density spectrum for BBHs assuming four evolution channels, isolated (Field), Young Star Cluster (YSC), Globular Cluster (GC) and Nuclear Star Cluster (NSC). Uncertainties, depicted by the shaded areas, are derived from the merger rates given in table 2 of [338]. The black dashed curve shows the sensitivity of ET for the triangular configuration.

(up to 30%). We also show the power-law integrated sensitivity curve of ET to stochastic backgrounds, computed for the triangular configuration and assuming SNR of 2 and 1 year of observing time with duty cycle of 50%. As discussed in [16], this sensitivity depends on the configuration: choosing two L-shaped detectors decreases the sensitivity above $\sim 100\,\mathrm{Hz}$ because the overlap reduction function drops significantly. However, L-shaped configurations where the detectors are co-aligned perform better at low frequencies than the triangular ones.

As can be seen in figure 82, the spectral shape at low frequencies is dominated by the inspiral phase of each BBH and therefore has a constant slope close to $f^{2/3}$. At higher frequencies, however, we start observing features specific to each formation channel that reflect the distribution of masses and redshifts of each population [2076, 2205]. In particular, the frequency at which the spectrum deviates from a power-law corresponds to the minimal mass in the BBH population (the peak is relatively wide due to redshifting effects). In figure 82, this deviation starts at a few hundred Hz for the Field formation channel, and at $\sim 100\,\mathrm{Hz}$ for the YSC and GC channels. Thus, observing the shape of the SGWB can provide important clues as to the formation scenario of the sources.

4.10.2 Study of Population III stars

As discussed in section 4.7.1, Pop III stars are the first stars that formed in the Universe. Similarly to Pop I/II stars, they form BBHs via the isolated or dynamical channels. However, Pop III remnants are expected to have unique properties that may help to distinguish them

JCAP03(2026)081

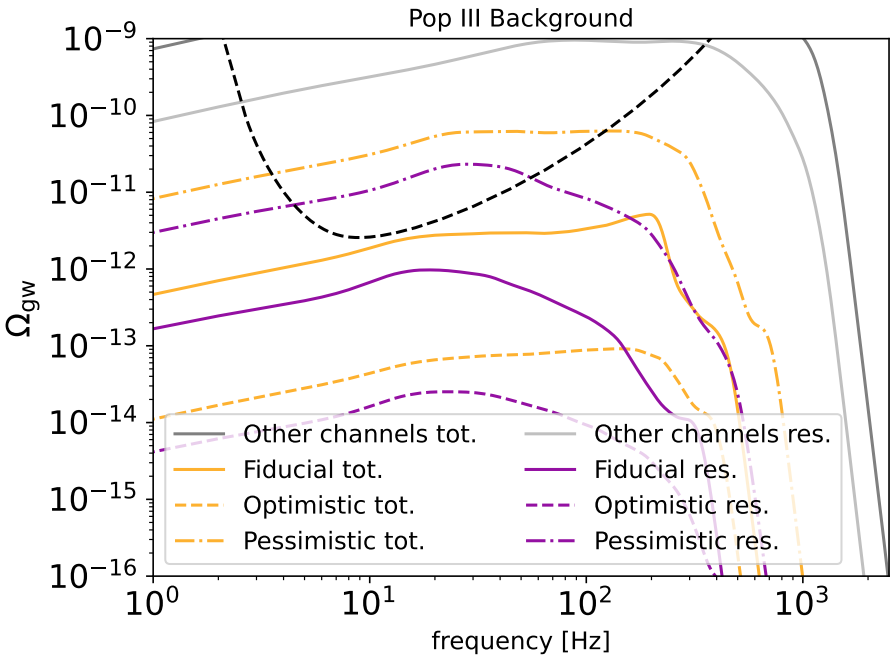

Figure 83. Background energy density spectra for BBHs born from Pop. III stars. Fiducial, Optimistic and Pessimistic models are the LOG_H22, LAR_H22 and LAR_J19 respectively populations models from [1674]. The residuals correspond to $\rho_{\text{thrs.}} > 20$, and the grey lines correspond to the background from Pop. I/II channels (see section 4.10.1).

from Pop I/II remnants, in particular merger rate evolution with redshift and mass spectrum. These properties are also imprinted on the SGWB they produce [2077, 2078, 2080, 2206].

As an example, in figure 83 we show the total and residual SGWB, where the source populations are taken from [1674]. The residual signal was calculated assuming all sources with an individual signal to noise ratio $\rho_{\text{thrs.}} > 20$ are subtracted noiselessly. Note that the SGWB from Pop III remnants starts deviating from a power-law at lower frequencies compared to Pop I/II remnants, as a consequence of their higher masses and higher merger redshifts.

We note that the residual signal form Pop I/II remnants in the model shown in figure 83 is more than two orders of magnitude above that of Pop III remnants due to their low merger rate. Therefore a better understanding of Pop III remnants is needed in order to efficiently extract information from the SGWB. Nevertheless, even if the residual Pop III signal is indeed much below the one from Pop I/II, SGWB observations will contribute to putting upper limits of high-z merger rates. In addition, the predictions for Pop III remnant merger rates and masses are much more uncertain that those for Pop I/II. Finally, we note that the ability to accurately subtract the signal from individually detected Pop III remnants highly depends on ET performance at low frequencies.

JCAP03(2026)081

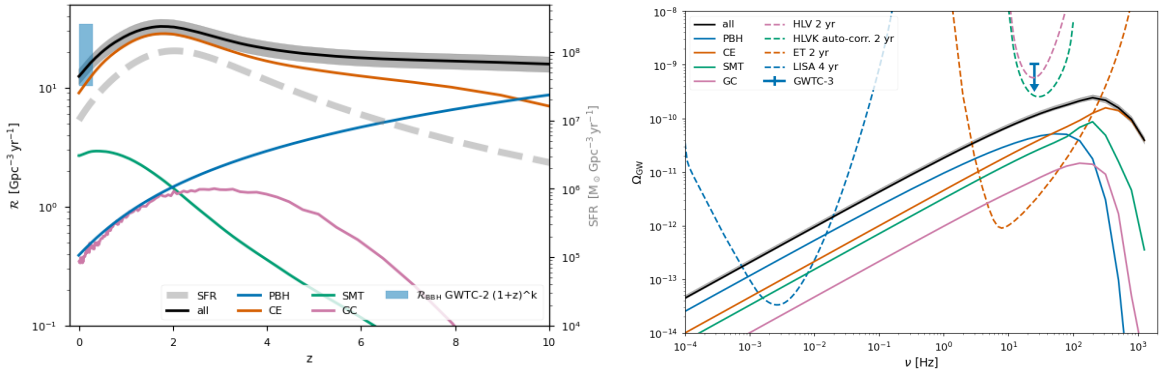

Figure 84. *Left panel:* merger rate evolution for representative astrophysical models and the PBH channel. As for the astrophysical models, CE, SMT, and GC refer to common envelope mass transfer, stable mass transfer, and globular clusters, respectively. The normalization comes from the Bayesian inference on the GWTC-2 catalog in ref. [1382]. The blue band reports the local merger rate bound from LVK while the dashed gray band the star formation rate (SFR). *Right panel:* total SGWB (black line) coming from the various channels shown in the left panel, while we report with colored lines their contributions. We do not show the residual SGWB. Figures adapted from ref. [2205]. Reproduced with permission from [2205]. S.S. Bavera et al., A&A, 660, 2022, reproduced with permission, © ESO.

4.10.3 Primordial black hole contribution

Primordial black hole mergers may lead to a sizeable SGWB [1922, 2205, 2207–2210].[44] As indicated in eq. (4.5), the SGWB results from the incoherent superposition of stellar and BH mergers, and it gets contributions from the entire merger history. In other words, it is sensitive to the rate evolution with redshift of the channels responsible for GW emission. Crucially, the PBH scenario is characterized by a merger rate that grows monotonically with redshift [1939, 1943, 1949] $\mathcal{R}_{\rm PBH}(z) \propto t^{-34/37}(z)$, extending up to early epochs at $z \gtrsim \mathcal{O}(10^3)$, see also discussion in section 4.6.1.[45]

In figure 84 (left panel), we show the merger rate distribution of PBHs as a function of redshift (blue line), compared to other representative astrophysical models both from isolated (common envelope, stable-mass transfer) and dynamical (globular cluster) formation scenarios from ref. [1570] (see [1382] for more details). The chosen normalization reflects the result found in ref. [1738] with a multi-channel Bayesian inference of the GWTC-2 catalog. While we do not discuss the mass distribution of the populations assumed in these plots, we highlight the large contribution from PBHs at low frequencies even if they only contribute to a subdominant fraction of the local merger rate density in this specific example. This property allows testing the presence of PBH binaries, adding an independent constraint to the model selection, as a cross-correlation between local rate and SGWB amplitude would provide valuable information on the merger rate distribution of the various channels at a relatively high redshift. The degeneracy between the PBH models and other astrophysical scenarios would then be broken by the fact that the former predicts a monochromatic growth

[44] The SGWB associated with the PBH formation mechanisms is discussed in section 3.2.5.1.

[45] We do not consider the contribution to the SGWB from PBH hyperbolic encounters, since it is typically subdominant [1938].

JCAP03(2026)081

of the merger rate density with redshift, thus the integrated SGWB would be larger for the same local (i.e. low redshift) observed rate.

4.10.4 Astrophysical Uncertainties in background description

While the recent detections of CBC by ground-based interferometers have provided a wealth of information on the BBH, BNS and NSBH populations, many uncertainties remain. These uncertainties can have an important impact on our predictions of the SGWB and can be divided into two categories: CBC source properties, which can be modelled with stellar models and constrained with current observations; and galaxy evolution, including SFH, Initial Mass Function (IMF) and metallicity evolution, which are taken from observations. On the other hand, observations with ET offer an opportunity to lift these uncertainties and thus obtain indirect constraints on these physical processes.

As was shown in [2211], uncertainties in the mass distribution of stellar-mass BBH affect not only the overall amplitude of the SGWB (see also [2212]), but also the spectral shape around the peak and the location of the peak. Moreover, current instruments are sensitive only to relatively low redshifts ($z \sim 0$ for BNS and $z \lesssim 1$ for BBH). Therefore in order to compute the SGWB we need to extrapolate our models up to $z \sim 10$. However, not only the merger rate may evolve with redshift, but also source parameters, such as mass distribution, which would strongly influence the SGWB, as shown in [2211].

Another major source of uncertainty is the SFH, which serves as the basis for SGWB modeling since it determines the total number of stars formed at each epoch [2202]. The SFH can be measured from the UV and IR luminosity functions of galaxies; however, in addition to various observational biases, such as dust attenuation, surveys often suffer from incompleteness at higher redshifts, beyond $z \sim 3$ (see e.g. [1249]). A closely related parameter is the IMF, which describes the number of *massive* stars formed in a given population. The IMF is typically assumed to be universal across environments and redshifts. However, some recent studies show that this may not be the case, which could strongly influence the number of compact objects formed and therefore the SGWB. Finally, the metallicity evolution is highly important for modeling the SGWB, since, as discussed in section 4.2, the efficiency of forming CBCs strongly depends on metallicity (see e.g. [1375, 1597, 2202, 2213]). The reason for this dependence is two-fold: first of all, stellar winds become stronger at high metallicity, and can remove a large fraction of the initial stellar mass before the star reaches core-collapse. This process leads to reduced masses of the resulting BHs. Second, metallicity can impact the efficiency of mass transfer phases during binary star evolution (like the common envelope phase), which can result in less efficient mergers and a lower probability of forming BBHs. In addition, metallicity influences the properties of supernovae that produce BHs through fallback. Measuring the metallicity evolution remains challenging, especially for $z \gtrsim 3$ (e.g., [1249]) and these observational uncertainties lead to large variations in the predicted SGWB [2076, 2211].

We expect several of these uncertainties to be lifted in the next few years: the number of detected CBCs is expected to increase, leading to a better determination of the mass spectrum; the reach of electromagnetic observations, in particular with JWST, is also extending, and a better measurement of the SFH at high redshift is foreseeable. Nevertheless, some of

JCAP03(2026)081

the open questions will remain until the deployment of ET, such as the mass distribution and merger rate of CBCs at high redshifts. The metallicity evolution and IMF universality also remain challenging targets to study. Thus, future observations of the SGWB with ET will help constraining not only the properties of CBCs but also several crucial aspects of galactic evolution. In this regard, studying the SGWB is complementary to the direct catalog approach: combining both resolved and unresolved populations will give the most complete picture of the compact binary evolution across cosmic times.

4.10.5 Sources other than CBCs

While CBC are the most studied class of GW sources, and the only one detected so far, other sources are expected to be detectable with ET, including stellar collapses and isolated neutron stars that are described in detail in section 8. Recent works have studied the SGWB produced by core-collapse SNe [2214, 2215] and rotating neutron stars [581, 2216]. In the case of core-collapse supernovae (CCSN), individual detections with ET would be possible only for the local Universe, whereas the SGWB includes also the contribution from more distant sources. Ref. [2215] studied a large range of CCSN explosion models and calculated the stochastic GW signal. They showed that for most models the expected SGWB is below the sensitivity of ET, with $\Omega_{\rm GW} \simeq 10^{-16}$ at $f \sim 10\,{\rm Hz}$ and $\Omega_{\rm GW} \simeq 10^{-14}$ at $f \sim 100\,{\rm Hz}$. The only exception are extreme models that feature rapidly rotating progenitors with a low ratio of rotational to gravitational potential energy that produces a rotational instability (low-$T/|W|$ instability). This instability produces strong GW emission between 200 and 300 Hz. Therefore, if a large fraction of CCSN progenitors share this property, the resulting stochastic background would be much stronger, with $\Omega_{\rm GW} \simeq 10^{-10}$ at $f \sim 200\,{\rm Hz}$ and possibly detectable with ET. It should be noted that such extreme models are considered unrealistic, since only a small fraction of massive stars are rapidly rotating. On the other hand, there are currently large uncertainties in the predictions of the GW signal from CCSN, and the resulting GW background differs by several orders of magnitude between models.

Rotating non-axisymmetric neutron stars also emit GW due to time varying mass quadrupole. This signal is expected to be much weaker than that of merging binary compact objects, but to last for much longer times. The loudest sources will thus be possibly detectable individually, but the contribution from unresolved sources will constitute a confusion background. This signal depends on the highly uncertain equation of state of neutron stars, their deformability, the distribution of rotation periods and magnetic fields (that contribute to the deformation of the star) and possible accretion from a companion. In ref. [581], the SGWB from rotating neutron stars was estimated as $\Omega_{GW} \simeq 2 \cdot 10^{-8}$ at $f = 760\,{\rm Hz}$, which would be potentially detectable with ET.

In both cases, CCSN and isolated neutron stars, the modeling uncertainties are still very large and accurate predictions are challenging. More theoretical work is needed, in particular in the areas of hydrodynamical simulations of core-collapse SNe and the nuclear equations of state of neutron stars.

JCAP03(2026)081

4.10.6 Anisotropies and cross-correlation with electromagnetic observables

The astrophysical SGWB is not perfectly homogeneous across the sky, but exhibits some level of anisotropy. As we already saw in eqs. (3.17) and (3.18), these can be addressed introducing a directional dependence in eq. (4.5), writing

$$\Omega_{\rm GW}(f,\hat{\boldsymbol{n}}) = \frac{1}{\rho_c}\frac{\mathrm{d}\rho_{\rm GW}(f,\hat{\boldsymbol{n}})}{\mathrm{d}\ln f\ \mathrm{d}\hat{\boldsymbol{n}}} = \bar{\Omega}_{\rm GW}(f) + \delta\Omega_{\rm GW}(f,\hat{\boldsymbol{n}})\,, \tag{4.7}$$

where $\hat{\boldsymbol{n}}$ is the direction of observation, $\bar{\Omega}_{\rm GW}(f)$ is the homogeneous component of the energy density, and $\delta\Omega_{\rm GW}(f,\hat{\boldsymbol{n}})$ is the anisotropic perturbation. The statistical properties of the anisotropies can be characterised in terms of the frequency-dependent angular power spectrum:

$$\langle \delta\Omega_{\rm GW}(f,\hat{\boldsymbol{n}})\,\delta\Omega_{\rm GW}(f,\hat{\boldsymbol{n}}')\rangle = \sum_\ell C_\ell(f) P_\ell(\hat{\boldsymbol{n}}\cdot\hat{\boldsymbol{n}}'), \tag{4.8}$$

where $P_\ell(\hat{\boldsymbol{n}}\cdot\hat{\boldsymbol{n}}')$ are Legendre polynomials. The SGWB anisotropies are generated by the intrinsic clustering of sources and the line-of-sight effects accumulated during the propagation through the large-scale structure [541–545, 547, 548]. Moreover, kinematic anisotropies arise from the motion of the observer with respect to the rest frame of the SGWB [556–558]. The theoretical expression of the SGWB anisotropies and their detection prospects have been subject of intense study in the last years; see section 3.1.2 for a review of this topic, for both the cosmological and astrophysical background components.

The astrophysical SGWB is given by the superposition of a large yet finite number of unresolved signals. In the ET band, the GW events from BBHs are expected to be separated in time and with a limited time overlap (while some overlap is expected for BNS mergers). Hence, the sources of the SGWB are discrete in space and time, and their number fluctuates according to a Poisson distribution, resulting in a significant shot noise. The total SGWB angular power spectrum is therefore $C_\ell^{\rm tot} = C_\ell + N^{\rm shot}$, where the shot noise contribution is flat in the ℓ-space and dominates over the intrinsic anisotropies. Indeed, the intrinsic anisotropies are typically at the level of $\delta\Omega_{\rm GW}/\Omega_{\rm GW} \sim 10^{-3} - 10^{-2}$ [546, 549–552], while the shot noise is around one order of magnitude larger [587–589, 1354]. Given the sensitivity of ET to various multipoles (see e.g. the analysis of [2217]) and the presence of shot noise, directly detecting the anisotropies due to clustering and line-of-sight effects will be extremely challenging. However, shot noise is expected to be measured with good precision, at least within the range of amplitudes predicted by most astrophysical scenarios. Despite being insensitive to the sky distribution of the sources, the shot noise still carries astrophysical information as its amplitude depends on the overall number of sources contributing to the SGWB and thus reflects the underlying astrophysics.

An effective way to overcome the shot noise issue is to cross-correlate the SGWB with electromagnetic observables. Indeed, the SGWB anisotropies are correlated with other cosmic fields that trace the large-scale structure, such as galaxy number counts [546, 549, 589, 1352, 1353], weak gravitational lensing [546, 549], CMB [578], and CMB lensing [1354]. All of these studies have shown that the SNR of the cross-correlation outperforms that of the auto-correlation by several orders of magnitude. Measuring the angular power spectrum of the cross-correlation between the SGWB and an electromagnetic observable can provide

JCAP03(2026)081

constraints on various astrophysical and cosmological quantities. Moreover, cross-correlating with a redshift-dependent observable (such as the number counts of galaxy, at different redshifts), allows one to have a tomographic reconstruction of redshift information, i.e. to extract the contribution to the total background from sources in a specific redshift band.

In [1353], the cross-correlation between LVK data and the Sloan Digital Sky Survey catalog was exploited to derive upper limits on a set of effective astrophysical parameters describing the local process of GW emission at galactic scales. As the sensitivity of the GW detector network improves, the approach presented in [1353] will become more effective, enabling more stringent constraints on the astrophysical kernel and its effective parameters. ET will improve the sensitivity to the angular power spectrum of the cross-correlation by more than a factor ~ 1000: ET is expected to reach and explore the astrophysically interesting region of the parameter space. Yet another approach could be to use the hierarchical Bayesian approach to estimate the BBH SGWB anisotropy [2218], which could also lead to ~ 1000 times sensitivity improvements relative to the approach presented in [1353], hence resulting in a very significant improvement when applied to ET data. This is a promising approach which might help to set stringent constraints on the parameter space of the underlying astrophysical models. The cosmological significance of cross-correlating the astrophysical SGWB with electromagnetic observables, such as measuring the bias of the SGWB and constraining non-gaussianities in the large-scale structure, is discussed in section 3.4.1.2.

Given a generic anisotropic signal, an important challenge is mapping its angular distribution [567]. For an unpolarized stochastic signal, the stochastic search with ET aims to reconstruct the SGWB power spectrum $S_h(f, \hat{\mathbf{n}})$ defined in eq. (3.11), while in the more general case of a polarized signal we want to reconstruct the quantity $H_{AA'}(f, \hat{\mathbf{n}})$ defined in eq. (3.8), which also includes the Stokes parameters describing circular and linear polarization. For most of the astrophysical backgrounds, the frequency and the angular dependence of the power spectrum of the SGWB in eq. (3.11) are factorized.[46] Then, restricting to the unpolarized case

$$S_h(f, \hat{n}) = S_h(f) E(\hat{\mathbf{n}}) \,. \tag{4.9}$$

It is then convenient to decompose the angular part of the power spectrum in spherical harmonics[47]

$$E(\hat{\mathbf{n}}) = \sum_{\ell=0}^{\infty} \sum_{m=-\ell}^{\ell} \delta_{\ell m} Y_{\ell m}(\hat{\mathbf{n}}) \,, \tag{4.10}$$

and then reconstruct the value of the anisotropic (map) coefficients $\delta_{\ell m}$ from the cross-correlation of the instruments' data streams that are available [640, 2222]. The reconstruction is performed in the framework of Bayesian analysis, by writing the likelihood function of

[46] Although Doppler anisotropies induced by the motion of the detector with respect to the rest frame of the SGWB induce a mixing between frequency and angular dependence, see [556]. For a more general treatment we refer to the formalism developed in [2219].

[47] The so-called pixel domain is an alternative basis that can be employed to decompose the angular dependence of the power spectrum [2220, 2221]. However, for the astrophysical and most of the cosmological models of a SGWB the spherical harmonics choice is the most natural one.

JCAP03(2026)081

the cross-correlators, expressing it as a function of the coefficients $\delta_{\ell m}$ and performing a maximum likelihood estimation, which can be done by a Markov-chain Monte Carlo (MCMC) or by a Fisher analysis.

Several factors may affect the quality of the reconstruction of the anisotropic map. Firstly, the instrumental noise puts a threshold on the detectability of the anisotropy coefficients δ_{lm}. In particular, the higher values of ℓ in the expansion of eq. (4.10) produce a signal in the high-frequency side of the power spectrum. This is due to the fact that the anisotropic overlap reduction functions of ground-based interferometers (which quantify the sensibility of a cross-correlator to a specific anisotropy) show a peak at a frequency $f \propto \ell b/c$, where b is the baseline between the pair of instruments taken into account.

Furthermore, up to today most of the map-making analyses have been performed for a Gaussian SGWB [100, 640], with stationary statistics in its reference frame. Under this assumption, the frequency domain is a natural choice to perform the data analysis.[48] The signal-to-noise ratio (SNR) grows with the square root of the time and it is dominated by the frequencies at which the overlap reduction functions, for each anisotropic coefficient of the map, display a peak. In fact, the astrophysical GW background is expected to be nonstationary due to the finite number of sources generating it [551, 587–589]. More sophisticated analyses that aim to work beyond the frequency domain must be employed if we want to tackle the challenge of extracting a weak anisotropic signal, as expected by both the astrophysical and cosmological models. A joint analysis of the SGWB along with the information given by the angular distribution of the resolved GW sources and the electromagnetic surveys will certainly help in that direction.

Another aspect that must be considered when studying the SGWB with ET (and in general in next generation detectors) is the nuisance effect due to the intrinsic variance of the signal [2223]. This effect impacts the measurement of the anisotropy coefficients in the limit where the instrumental noise is lower in absolute value with respect to the total effect of the SGWB on the interferometers. In fact, the current analyses work in the opposite regime, i.e. the so-called noise-dominated assumption. It has been shown [640] that current detectors live in the noise-dominated regime, while for ET and the new generation interferometers, the intrinsic variance of the signal will no longer be a negligible effect when compared to the low instrumental noise power spectrum.

As a last important remark, the mapping of the high ℓ values for the SGWB angular power spectrum and all the odd ℓ values is suppressed when the baseline between the instruments is small. This results in enhanced sensitivity for the proposed configuration [16] of 2 L-shaped Einstein Telescopes in two different sites, improving the detectability for those anisotropies of several orders of magnitude with respect to the original triangular-shaped design. In a similar way, the analysis obtained by cross-correlating ET with other new-generation instruments (such as Cosmic Explorer) will result in a significantly greater sensitivity to the SGWB anisotropies.

[48]The rotation of the Earth results in an observed GW background which is cyclo-stationary in the reference frame of the detectors. In [640, 2222] a folding method is employed in order to take into account this effect in the data analysis process.

JCAP03(2026)081

4.10.7 Spectral shape reconstruction

As already mentioned in section 4.10.2, the SGWB spectral shape contains plenty of information on the underlying astrophysical populations from which the sources responsible for the SGWB generation are drawn. Techniques for SGWB spectral shape reconstruction are thus crucial for extracting this information from the data. While it is known that the astrophysical background is not perfectly isotropic, stationary, or unpolarized (see, e.g., [546, 551, 582–584, 587, 589]), in the remainder of this section, we neglect these features and focus on the spectral shape only. In this limit, all the information on the SGWB is contained in the function $S_h(f)$ in eq. (4.9), which fully characterizes the spectrum. This quantity is uniquely determined, through eqs. (3.13) and (4.5), by the population properties, and inherits the dependence on the population (hyper)parameters, say Λ_i. These (hyper)parameters characterize, among others, the mass function and the merger rates for all the subpopulations contributing to the SGWB, and impact the overall amplitude and the position and sharpness of the high-frequency cutoff in the frequency spectrum [2205, 2224].

In a consistent Bayesian approach, all the Λ_i would have to be included in the analysis, and their parameter space would have to be sampled simultaneously.

There are several challenges to be faced while following the above procedure in the context of ET. For example, since several components contribute simultaneously to the overall signal, the dimensionality of the parameter space may be significant (if not prohibitive), and all signal components will effectively act as an additional nuisance to each other. Sampling such a parameter space, which might be highly degenerate and non-Gaussian, can be quite a non-trivial problem from a numerical point of view. For this reason, an alternative (and computationally less demanding) avenue could be to separate the data analysis problem into two steps. In an initial step, one would attempt an agnostic reconstruction of the SGWB spectrum (for some techniques developed in the context of LISA data analysis, see, e.g., [644–647, 2225, 2226]) to capture the overall frequency shape. In a second step, the constraints on the spectrum are converted into constraints on the population (hyper)parameters. Such an approach has the merit of compromising between accuracy and feasibility, and it could be used, e.g., to identify the relevant part of the parameter space to be sampled with the full Bayesian techniques described in the previous paragraph.

4.11 Executive summary

Here we summarize the advancements that ET will bring in population studies and astrophysical backgrounds, in comparison to the current state of the art, specifically emphasizing the distinct features that the ET will allow us to explore. The following are the major areas where ET's capabilities surpass the current generation of GWs detectors.

Astrophysical CBCs across cosmic time

- **Formation channels.** Current models describe a remarkable zoo of CBC formation channels, including (stable and unstable) mass transfer in massive binaries, chemically homogeneous evolution, dynamics in star clusters and gas rich AGNs. With the prospective detection of 10^5 BBH and BNS events per year, it

JCAP03(2026)081

will be possible to characterise in detail the impact of the isolated and dynamical channels on the formation of CBCs. This can be achieved by constraining crucial quantities like merger rates, redshift dependencies, masses and spins of merging CBCs.

- **Merger rate density evolution.** Current detectors enable us to infer the merger rate density of BNSs and BHNSs at redshift zero, and to reconstruct the BBH merger rate density up to a redshift of $z \approx 1.5$, under several assumptions. ET will be a paradigm shift for measuring the merger rate evolution of astrophysical CBCs: we will estimate the intrinsic BBH merger rate up to a redshift of $z \approx 100$ and the BNS merger rate at least up to cosmic noon. This will yield unique opportunities to constrain the formation of CBCs, their possible dependence on stellar metallicity, their delay time, the evolution of their stellar progenitors, and the link with their host galaxies.

- **CBC masses.** From current detections, several peaks have already emerged in the mass function of primary black holes. ET will not only constrain these features to an exquisite level of accuracy, but will also probe their evolution with cosmic time and the existence of the claimed pair-instability mass gap.

- **CBC spins.** Current gravitational-wave data suggest a tension between the spin of black holes in gravitational-wave detections and X-ray binaries. Our ability to interpret this claimed tension in terms of formation history of X-ray and gravitational-wave black holes is hampered by large observational uncertainties. Moreover, hierarchical merger models predict a peak of the precessing spin at $\chi_{\rm p} \sim 0.7$ for second-generation black holes. ET will yield an accurate reconstruction of the spin distribution of black holes, providing a conclusive answer about the claimed tension and the existence of moderate to high-spin peaks.

- **Population III stars.** ET will yearly observe between 10 and 10^4 binary black hole mergers from the first generation of stars that appeared in the Universe (Population III stars). The main challenge will be to disentangle such population from primordial black holes and black holes born from other stellar progenitors.

- **Intermediate-mass black holes.** Intermediate-mass black holes are crucial to explain the formation of supermassive black holes observed at the center of most galaxies, but have largely eluded our efforts to characterize them with electromagnetic surveys. GW190521 demonstrated the potential of gravitational-wave detectors to probe the intermediate-mass black hole regime. ET will enable us to study a rich population of intermediate-mass black holes, up to a redshift $z \approx 10$. This will offer unique opportunities for multi-band gravitational-wave observations with space-based detectors.

JCAP03(2026)081

Primordial Black Holes

PBHs are BHs which could have formed in the early universe and might compose a non negligible fraction of the dark matter. ET will allow to pin down the presence of PBHs to unprecedented precision through its capability to search their GW signatures. On one side, thanks to its superior sensitivity and wider bandwidth at low frequencies, ET will test the unique feature of the PBH merger rate density, its monotonically increase with redshift, up to redshifts larger than 30 where astrophysical sources are not present. Secondly, ET will drastically improve the sensitivity leading to a possible detection of subsolar PBHs, a smoking gun for their existence given the fact that subsolar astrophysical BHs may not exist.

Population backgrounds

- **Sources.** Most BBHs can be detected individually by ET. However, using a background approach for parameter reconstruction is valuable for cross-checking results against catalog data, as any discrepancies may indicate faint subpopulations that individual analyses might miss. For BNSs, the bulk of the population will be sub-threshold, and a background study provides insights that catalog approaches cannot offer. ET is also expected to detect sources other than CBCs, such as stellar collapses and isolated neutron stars (see section 8). Finally, a population of PBHs extends at redshifts beyond ET's detection horizon, making a background approach crucial for studying them.

- **Astrophysical information.** Different formation channels for BBHs will influence their masses, spins, and eccentricities, as well as the merger rate, distribution of time delays, and the evolution of the mass spectrum with redshift. These variations are expected to be reflected in the stochastic gravitational wave background (SGWB) observable by ET. Pop III remnants are expected to possess unique characteristics that could be detected in the SGWB they generate.

- **Detection prospects.** The angular power spectrum of the cross-correlation between the SGWB and electromagnetic observables is a promising observable for a first detection of anisotropies. ET is expected to enhance sensitivity to this angular power spectrum by over a factor of approximately 1000, allowing access to astrophysically significant regions of parameter space. Similar improvements are expected from the hierarchical Bayesian approach.

- **Mapping.** The configuration of two L-shaped detectors at different sites greatly enhances the detectability of anisotropies compared to the triangular design. Moreover, cross-correlating ET with new-generation instruments like Cosmic Explorer will further improve angular sensitivity to the SGWB.

- **Spectral shape.** An agnostic reconstruction of the frequency shape allows converting constraints on the spectrum into limits on population (hyper)parameters.

JCAP03(2026)081

5 Multi-messenger observations in the ET era

The cosmological reach of the Einstein Telescope is such that it will detect extremely large numbers of compact object mergers which should also create luminous electromagnetic counterparts. If successfully paired, this can lead to substantial samples of multi-messenger sources that can be used to understand heavy element nucleosynthesis, probe physics at high density and extreme velocity, measure cosmological parameters, and constrain alternative theories of gravity. These objects will typically lie in the mid-to high-redshift Universe, and so while their detection in gravitational waves may be straightforward, we must enhance and optimize our electromagnetic capabilities if we are to exploit the treasure trove of scientific results that can flow from multi-messenger observations. Here we review the likely signatures occurring in coincidence with ET-detected mergers. We construct both population models and up-to-date implementations of the emission physics for electromagnetic counterparts to determine their recovery with both electromagnetic and neutrino facilities that may be available in the 2030s. We highlight the requirements of localisation capability, and that EM capability should be co-developed along with ET to ensure that the critical science questions enabled by multi-messenger observations can be answered.

5.1 State of the art

5.1.1 Multi-messenger Astronomy

Traditionally, we have studied the Universe with light, from millennia of observations with the naked eye to the insights enabled by the discovery of the telescope and its continued refinement. In the 20th century, astronomers made spectacular progress with the development of multiwavelength astronomy. Multiwavelength astronomy led to the realisation that physical conditions in the Universe enabled some astrophysical sources to emit light across the electromagnetic spectrum. A myriad of astrophysical insights stem from multiwavelength observations, from the cosmic microwave background [2227] and its many applications [591] to new exotic source classes, including the radio-emitting pulsars [2228] and the high-energy dominated gamma-ray bursts [2229].

Throughout the twentieth century, there was also a realisation that distant astrophysical sources may also create signals that are not electromagnetic in origin. The journey to understanding these alternative carriers of information (messengers) began with the discovery of cosmic rays in 1912 and flows through solar neutrinos in the 1960s [2230] to the increasingly complex and sophisticated detectors for gravitational waves, which discovered the first sources in 2015 [1].

Multi-messenger astronomy is the combination of two or more of these astrophysical messengers, although one of these is typically electromagnetic light. The value of such detections is immense; the non-photonic messengers often carry information from regions that are essentially invisible to light. Gravitational waves cannot be shielded and so provide information about the behaviour of mass in kilometre-sized regions where compact objects such as neutron stars and black holes merge. Neutrinos can escape from the cores of collapsing stars, hidden from electromagnetic view by the star itself. Therefore, multi-messenger astronomy provides a direct probe of matter in conditions far exceeding those available in any Earth-bound laboratory. Strikingly, many objects that emit panchromatic electromagnetic light

JCAP03(2026)081

are also likely to be multi-messenger emitters, and this combination of messengers is critical both in studying the full details of the events in question and in using them as probes of extreme astrophysics and cosmology (see figure 85).

The first multi-messenger detection was of thermal neutrinos, coincident with SN 1987A in the Large Magellanic Cloud [2231]. However, supernovae neutrinos have not been seen in the 35 years since, despite the substantial improvements in detectors. The gravitational wave multi-messenger era began in 2017 with the discovery of gravitational waves from the binary neutron star merger GW170817 [2] and its subsequent identification from the gamma-ray to radio regime [4]. This detection enabled a raft of new scientific insights, which we describe in detail in section 5.1.2. To date, there has yet to be a further gravitational wave-electromagnetic source, despite intensive efforts. These endeavours will likely unveil further electromagnetic counterparts as the current generation of interferometers reaches their design sensitivities in the next few years. However, the rates of such detections mean that building samples beyond a handful of events will be challenging, and these events will all be at low redshift, ideal for detailed study of extreme physics in compact objects but of less utility in understanding source evolution or in deriving cosmological parameters.

Large samples of electromagnetic bright sources will require next-generation gravitational wave detectors such as the Einstein Telescope (ET), whose astrophysical reach is sufficient to uncover populations of thousands of likely electromagnetically bright events. This dramatic rate increase is possible because of the increased horizon of ET. It comes at the cost that the events will be more distant and will require novel approaches for their identification and characterisation, combined with the next generation of electromagnetic observatories that will be active in the 2030s. The realisation of the multi-messenger promise of ET will rely on developing electromagnetic capability in tandem with the gravitational wave detectors.

This section outlines the science enabled by multi-messenger observations. It reviews the progress made to date via studies of both GW170817 and similar systems, perhaps seen so far only in electromagnetic light. We subsequently construct detailed source population models to make predictions for both the rates of events and, critically, the expected electromagnetic signals. We then use these, along with a census of likely telescopes available to the community in the mid-2030, to make robust, if broad, predictions for the recovery of electromagnetic counterparts.

5.1.2 GW170817

To date, there is only a single unambiguous event in which gravitational waves and electromagnetic light have been observed in tandem, GW170817 [2, 4]. This binary neutron star merger provided an exceptionally rich set of data that continues to provide new scientific insight. Observations of GW170817 hence offer a template for what future observations may enable and also an opportunity to learn lessons and improve follow-up.

Both the LIGO detectors detected GW 170817, while an upper limit from VIRGO was decisive in breaking location degeneracies and providing an error box of only ~ 30 sq. degrees [4]. Only 1.7 seconds after the merger of the two neutron stars, a short-duration gamma-ray burst, GRB 170817A, was also detected by both the Fermi [2171] and INTEGRAL [2172]

JCAP03(2026)081

satellites. The rate of short GRB detection by these satellites is approximately one per week, so the time coincidence alone made identifying the GRB a highly significant event.

The source location was non-optimal for electromagnetic observations, lying only $\sim$ 50 degrees from the Sun, with very limited possibilities for follow-up. This location was also not promptly visible to any observatories at the point at which it was disseminated. Targeted electromagnetic observations did not begin immediately, but several hours later, when observatories in South America could observe the sky localisation, and the *Swift* satellite started its search [2232]. These searches were rapidly successful, with [2174] reporting a new transient, subsequently named AT2017gfo, in the galaxy NGC 4993 in observations taken 11 hours after the merger. Indeed, before this first announcement, five more observatories had also observed the source [2175, 2233–2236]. Initially, it was unclear if this source was related to GW170817 or was an unrelated supernova explosion. However, imaging and spectroscopy over the next 48 hours revealed a spectral evolution unlike any previously observed transient and cemented the association [2176, 2179, 2237–2239]. This spectral evolution was extremely rapid, with the source spectrum moving from a spectral peak at $\sim$ 5000Å to $\sim$ 15000Å on a timescale of only a few days. Strikingly, this signature was qualitatively extremely similar to what had been predicted for kilonova emission [2240, 2241], in which the high opacity of heavy elements synthesised in the explosion effectively blocks the optical light. IR and optical observations of the source continued for as long as allowed by the encroaching Sun, and on a timescale of 10–20 days, the counterpart was also detected in both X-ray [2173, 2242] and radio [2243] observations. Indeed, while a faint source was detectable by the Hubble Space Telescope 100 days after the merger [2244], the X-ray and radio afterglows continued to brighten, reaching their peaks on timescales of hundreds of days before decaying [2245–2248].

The comprehensive observational campaign for GW170817 led to a myriad of scientific advances, which we highlight below.

5.1.2.1 The kilonova and the origin of the heavy elements. The optical and IR light created in GW170817 was caused by the decay of newly synthesized elements in the merger. During the merger, neutrons are ejected both in tidal tails from the merger and a range of additional processes, such as the wind from a newly formed accretion disc. These neutrons then undergo neutron capture reactions via the so-called r-process, which builds extremely neutron-rich nuclei far from the valley of stability [2249]. The energy released as these unstable isotopes decay then powers the faint and fast transient that we know as a kilonova [2241] while also populating the high-mass regions of the periodic table. Indeed, it is thought that the r-process is responsible for the creation of around half the elements heavier than iron and is the dominant source of elements with significant social, geological, and even biological importance, such as gold, thorium, and iodine.

Before the discovery of GW170817 and its associated kilonova (AT2017gfo) several candidate kilonovave had been uncovered in the afterglows of (short) GRBs [2250, 2251]. However, AT2017gfo is by far the best-studied event, with a comprehensive set of both imaging and spectroscopic observations that are outlined in figure 87. These observations provide strong evidence for the production of r-process elements.

The abundance patterns of heavy elements show three apparent "peaks", often referred to as the first, second, and third peak elements. These are broad regions of higher elemental

JCAP03(2026)081

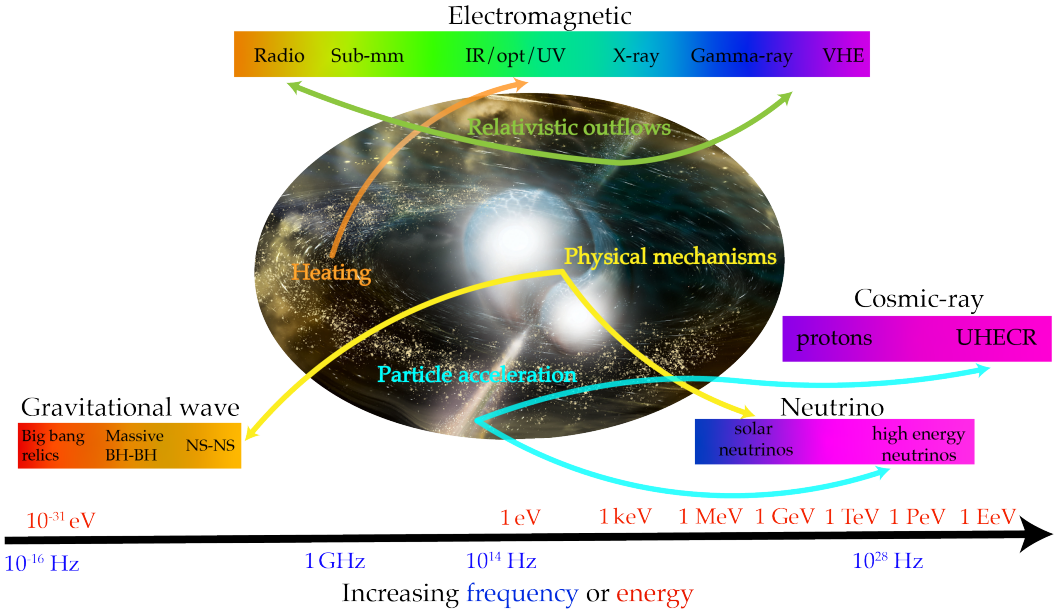

Figure 85. The promise of multi-messenger astrophysics. While much astronomy to date has been undertaken in the electromagnetic bands, in particular in optical light, many extreme systems in the Universe emit light across the electromagnetic spectrum and also produce additional messengers in the form of cosmic rays, neutrinos, or gravitational waves. Understanding the details of these systems and the insight they offer into central questions in astronomy, cosmology, and fundamental physics is something that can be done via multi-messenger observations.

abundance centered at atomic numbers around krypton (atomic number 36, first peak), xenon (atomic number 54, second peak), and platinum (atomic number 78, third). The production of elements around each peak depends on the nuclear physics ongoing within the material forming the heavy elements (in the case of a compact object merger, this is the ejecta). In particular, different nucleosynthetic pathways are available depending on how neutron-rich the material is. Perhaps counterintuitively, the neutron-richness of the ejecta is defined by its so-called electron fraction (Y_e), which is equivalent to the proton-fraction for material that is neutral on a bulk scale. In broad terms, access to the more massive elements becomes increasingly straightforward for decreasing Y_e. In general, the production of material in the second and third r-process peaks is thought to require $Y_e < 0.15$ [2241].

Within the merger of a binary system of neutron stars, or a neutron star with a black hole, material can be ejected via various mechanisms. Firstly, the initially less massive object is larger and will be tidally stretched and disrupted as the gravitational wave-driven inspiral reaches its final phases. Material from these (or plausibly both) stars is ejected in the plane of the orbit in so-called tidal dynamical ejecta. Having been stripped directly from a neutron star, this material is extremely neutron-rich and should be able to undergo r-process reactions to the most massive elements. As the merger proceeds, the vast majority of the total mass remains with the stars and, ultimately, the central merged object. However, some also form a disc around this object. This disc may be a source of r-process synthesis itself [2253], and also drives a wind which creates further ejecta in the polar directions. Because of strong radiation

JCAP03(2026)081

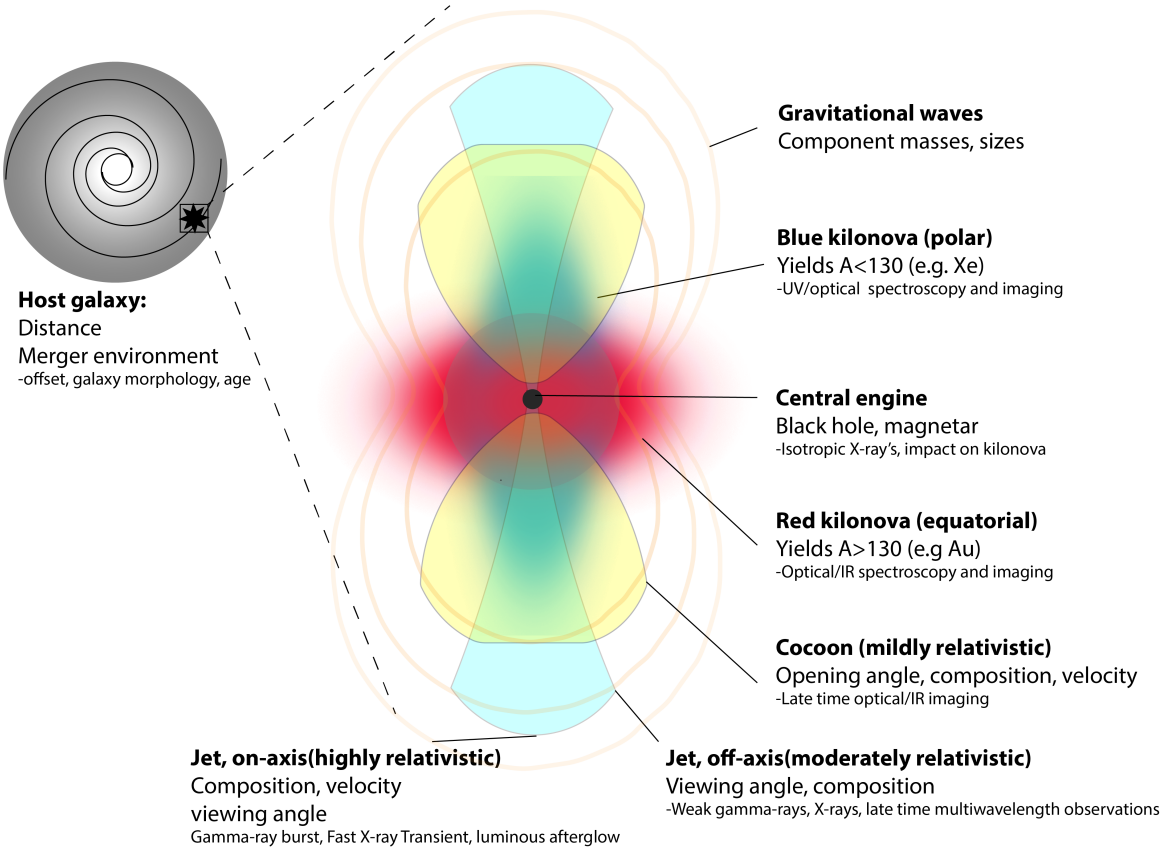

Figure 86. The physical process ongoing in the merger of a binary system of neutron stars (or a neutron star and a black hole), their multi-messenger observational signals and the scientific insight enabled from them (updated from an original concept by [2241]). Gravitational wave observations provide robust measurement of the component masses, and constraints on their sizes and spins. Many possible electromagnetic signals are also possible, including the detection of associated GRBs, cocoon emission, and kilonova signatures. Reproduced from [2241]. CC BY 4.0.

from this disc (in particular in the form of neutrinos which trigger inverse beta-decays), the material in this polar ejecta is less neutron-rich than in the tidal ejecta and likely yields intermediate mass elements around the first r-process peak.

While the elemental abundances within the ejecta are determined by nuclear physics, the observed light in the kilonova is determined by the atomic physics of the newly synthesized material. While this atomic physics, and in particular the energy levels of a given isotope, are well known for low-mass elements, there are substantial gaps and uncertainties for the most massive nuclei due to the immensely complex electron structures. Of particular importance for the appearance of kilonovae are the so-called lanthanides and actinides that have open electron f-shells, and extremely high numbers of electron transitions throughout the UV and optical region. The effect of this is to provide extremely high opacity to outgoing light rendering kilonovae which produce these elements extremely red [2240].

This work, much of which was undertaken prior to the discovery of AT2107gfo (but has been refined since), provided a broad expectation for what a kilonova should look like. It will

JCAP03(2026)081

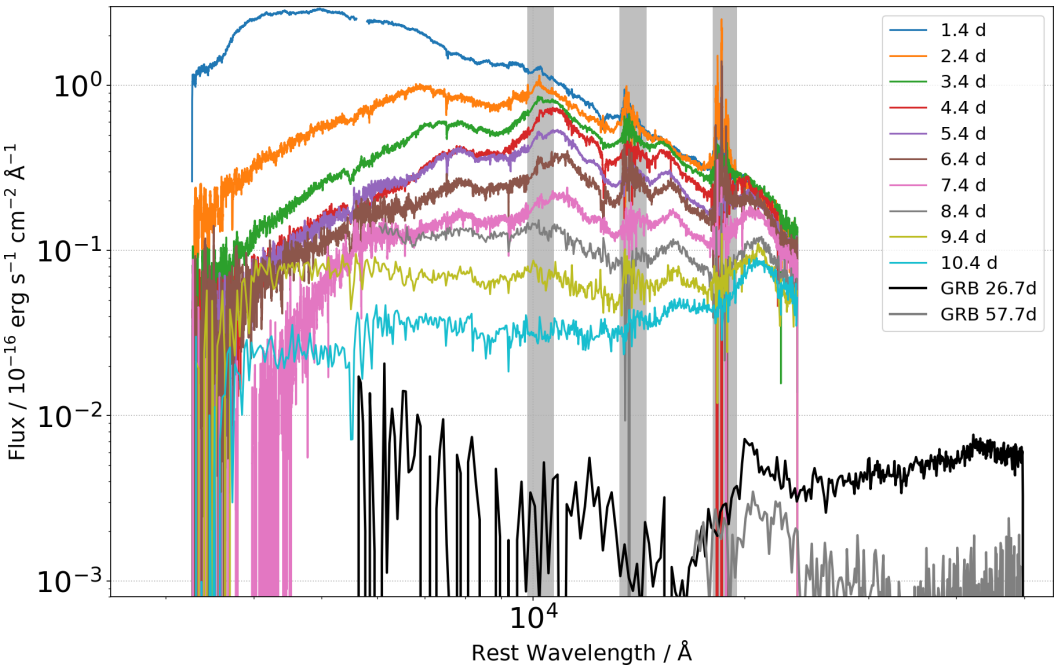

Figure 87. The spectroscopic evolution of kilonovae. The upper (colored) lines show the X-shooter spectral sequence for AT2017gfo [2179, 2237], demonstrating the early blue emission with the subsequent transition to a much redder spectrum. The lower (grey/black) lines show much later time spectra of the kilonova in GRB 230307A (AT 2023vfi) obtained with *JWST* [2252]. The spectra contain numerous spectra features both early in absorption and later in emission, and these have been linked to several different r-process elements.

have a low luminosity at peak (compared to most transients), evolve quickly because of the low ejecta mass, and either be very red or transition from blue to red on a timescale of a few days.

In bulk terms, this is exactly what was observed in AT2017gfo, and it was the similarity of the observed properties to the pre-existing theoretical predictions that gave strong evidence that AT2017gfo was indeed the counterpart of GW170817. However, it is also true that when investigated in detail there were many aspects of the observed event that did not match the models, and demonstrated the requirement of more sophisticated approaches to fully exploit the potential of kilonovae in probing heavy element enrichment. In part, this explains why continuing analysis of the AT2017gfo observations reveals new insight 7 years after its discovery. Indeed, the kilonova, AT2017gfo has been the most widely studied component of GW170817, with several hundred articles dedicated to its study. While many of these studies disagree on the details of the source, often because of the use of disparate sets of models, the broad picture appears to be generally agreed upon. The source emitted in the range 0.02–0.1 $M_\odot$ of r-process material [2176, 2179, 2181, 2233, 2235, 2237, 2254]. The composition of this material is a mixture of lighter r-process elements which are responsible for the early bluer emission, and heavier elements, responsible for the redder, later emission [2254, 2255].

Most the these conclusions are drawn from the study of the multi-wavelength lightcurves of the kilonova. However, very substantial effort has also gone into the evolving spectral series, which shows significant variations, even on the sub-hour timescale at early times [2256].

JCAP03(2026)081

These observations reveal the presence of strontium at early times [2257], an identification now generally agreed upon in the community [2258] and supported by theoretical expectations [2259]. These early observations also potentially contain several further spectral features, such as yttrium [2260], although the challenge in such identifications is substantial given the uncertainties in the atomic physics of heavy elements.

There has also been substantial interest in the later phases of the spectrum, which because of the low ejecta mass and high velocities rapidly become optically thin. At this point, it is plausible that emission lines may be observed. In the later IR spectra of AT2017gfo a prominent line at 2.2 microns has been interpreted as tellurium [2261, 2262], a line also seen in the JWST spectrum of a further KN in a GRB [2252, 2262].

The rich dataset for AT2017gfo continues to be exploited as models improve. The complex spectral and temporal evolution of the kilonova provides the opportunity to dissect the details of its composition and ejecta mass, although are currently limited substantially by model uncertainties. As these improve it should be possible to robustly infer the contribution of kilonova to the heavy element budget of the Universe. However, doing so concretely is likely to require samples of tens of kilonovae to understand source diversity and pinpoint rates. The current paucity of detections means that it is unclear if such observational samples can be built in a reasonable time with the current generation of gravitational wave detectors.

5.1.2.2 The gamma-ray burst and its afterglow. In addition to diagnostics from the core of the merging binary, electromagnetic observations also probe the relativistic outflow that created the GRB. In particular, GW observations (in particular when combined with the EM distance to the galaxy) provide a route to measuring both the energetics of the outflow, the inclination angle, and the structure of the relativistic jet. These provide substantial insight into the physics of GRB jets, as well as potentially into larger physics questions relating to the acceleration of material to ultra-relativistic velocity.

GRB 170817A was observationally a rather typical, if faint, short duration GRB, with a duration of $T_{90} = 2.0 \pm 0.5$ [2171] and a spectral shape consistent with that seen for other GRBs. In the absence of a distance measurement, it would not have stood out as exceptional. However, at a distance of only 40 Mpc the inferred energetics of the GRB are at the extremes of the distribution. In particular, the so-called isotropic equivalent energy release (the energy from the burst on the (false) assumption that it emits equally in all directions) is $E_{iso} = 10^{46}$ erg [2171, 2172]. This is four orders of magnitude lower than typical for short-GRBs [1652, 1653], which are typically found at much larger distances (these closest short-GRB after GRB 170817A is GRB 080905A at $z = 0.125$, or ~ 600 Mpc [2263], a factor of > 15 more distant than GRB 170817A, although there are some merger-related GRBs likely at lower redshift).

This likely explains why GRB 170817A was so underluminous compared to the bulk of the short GRB population — it was viewed off-axis. In turn, studies of the GRB afterglow provide a route to studying the jet structure and imply that the jet in GRB 170817A was highly structured, with a lower Lorentz factor in the wings, but a luminous, highly collimated event to an on-axis observer [2244, 2246, 2247, 2264–2267]. Indeed, in the years following the merger, deep observations utilizing radio interferometry [2268, 2269] and the *Hubble Space Telescope* [2270] could directly resolve the motion of the relativistic GRB jet. The implication

JCAP03(2026)081

is that GRB 170817A was viewed ~ 25 degrees from its jet-axis. It was an extremely faint afterglow, only just detectable to the premier facilities in the X-ray (*Chandra*/*XMM-Newton*), optical (*HST*) and radio (JVLA). Indeed, it may be that multi-messenger observations are one of the most effective routes of identifying GRB jets off-axis, and in doing so to study the structure of the GRB jets, itself of great importance in understanding the details of ultra-relativistic motion and particle acceleration.

5.1.2.3 The host galaxy and environment. In addition to the light from the transient itself, we can also glean much information about a given event from the environment in which it is born. Indeed, early in the history of studies of supernovae, it was apparent that type II events occurred exclusively in young, star-forming galaxies, while SN Ia also occurred in older populations, implying different progenitor systems. There is now a long history of using the environments of supernovae, gamma-ray bursts [1653, 2271–2277] and other transients [2278–2280] as a route to understanding the stars that form them.

The host galaxy of GW170817/AT2017gfo is NGC 4993, a massive lenticular galaxy. This has also been studied in great detail on both the scale of the galaxy [2167, 2168, 2170, 2281], and the local environment [2167, 2282]. These studies generally concur that the host galaxy is dominated by an old stellar population (> 1 Gyr, [2167, 2281, 2283]), with evidence for minor merger tens of millions of years ago [2170, 2284]. The vast majority of the stellar mass resides in the older populations, suggesting it is most likely the binary was formed in this population [2285]. There is no evidence for any underlying globular cluster to limits that probe the majority of the globular cluster luminosity function [2170, 2244]. In principle, observations of these locations are highly diagnostic of progenitor production, natal kicks, and delay times, since the host of GW 170817 is much closer than those of short GRBs for which such studies are typically undertaken [1653, 2286, 2287]

5.1.2.4 Tests of cosmology and fundamental physics. Observations of GW170817, GRB170817A, and the kilonova AT2017gfo enabled a unique route of probing the extreme physics at play in compact object mergers. For example, gravitational wave observations measure (or place constraints) the so-called tidal deformability of the neutron stars during the merger. The degree of deformability places restrictions on plausible equations of state (or mass-radius relations) for the matter at nuclear densities within neutron stars [2288]. Consistency checks on the results from these analyses can be run in tandem with electromagnetic observations; for example, are the allowed equations of state consistent with the mass ejected in the kilonova, or even how the equations of state rule in (or out) via tidal deformability studies compare with those inferred for different neutron stars via high-resolution X-ray spectroscopy of millisecond pulsars [2288, 2289].

A critical use of combined EM and GW observations is a novel one-stop route (distance ladder independent) to measure cosmological parameters. In particular, the waveforms of merging compact objects encode their masses and are so-called standard sirens [1138], where the measurement of the gravitational wave amplitude directly provides the distance to the source. The Hubble constant can be determined if paired with a measure of the velocity, for example, in the form of a redshift of either the electromagnetic counterpart or its host galaxy. For GW 170817, initial estimates were of $H_0 = 70^{+12}_{-8}\,\mathrm{km\ s^{-1}\,Mpc^{-1}}$ [1709], but improved

JCAP03(2026)081

to $H_0 = 71.9 \pm 7.1\,\mathrm{km\ s^{-1}\,Mpc^{-1}}$ [2290] using improved estimates of the distance to NGC 4993 or to $H_0 = 70.3^{+5.3}_{-5.0}$ via the determination of the inclination angle due to superluminal motion measurements of the GRB afterglow [2291].

Finally, the joint observations can constrain core questions in fundamental physics. In particular, the time delay between the gravitational waves and the first electromagnetic emission provides robust tests on any deviation between the speed of gravitational waves and the speed of light, which are several orders of magnitude better than previously available, suggesting any variations are smaller than one part in $\sim 10^{15}$ [3]. In turn, this rules out numerous alternatives to General Relativity which predict a difference between the two speeds. While more complex scenarios remain plausible (e.g., frequency-dependent speed of GWs), the observations are a strong demonstration of the ability to multi-messenger observations to pose new tests for the validity of General Relativity.

5.1.2.5 Limits on other messengers associated with GW170817. GW170817 was the first source to be identified in both gravitational waves and light, but there is also significant interest in the prospect that it also created further messengers, such as high-energy neutrinos accelerated in the relativistic jet. Several such searches were undertaken using time windows around GW170817 including both close to the merger time [2292] and over a much longer ~ 2 week time frame [2293]. The detection of such neutrinos would be a major step forward in our understanding of the details of particle acceleration in compact object mergers, although despite the relatively close distance to GW170817 the limits were generally significantly shallower than expected for the majority of models [2293, 2294].

5.1.3 GRBs and KN as counterparts of compact binary mergers

While we have, to date, only uncovered one electromagnetic counterpart of a binary neutron star merger detected in gravitational waves, we likely studied hundreds of such events in electromagnetic light only. In particular, the detection of a GRB in GW170817 strongly links at least some short-duration gamma-ray bursts to the mergers of compact objects. Indeed, this joint detection cemented a growing body of evidence that already linked short-GRBs to such mergers. For example, the host galaxies of the bursts appear to span a broad range of ages, from young, star-forming dwarfs to giant ellipticals [2295]. Such a broad range of ages is inconsistent with any origin in young, massive stars. Furthermore, the locations of the short-GRBs in and around their host galaxies were very different from that seen in long-duration gamma-ray bursts [2272] or in supernovae [2275]. In particular, a substantial fraction of short-GRBs arise at large offsets from their host galaxies [2296–2298], making it difficult to explain their locations without invoking progenitors that have received some kind of "kick" (though see [2299, 2300]). Such kicks are naturally expected to occur in compact object systems in which the combination of mass loss at the time of supernova (the so-called Blauw-kick) and natal kicks to neutron stars on formation [1665, 1666] can propel the binary from its birth site at tens to hundreds of km $\mathrm{s^{-1}}$. Finally, the first suggestions of kilonova emission were in the short-GRB 130603B [2250, 2251] and several possible examples had been uncovered before 2017 [2301, 2302]. Combined, this evidence suggests that many, if not all, short-duration GRBs arise from compact object mergers and provides us with a much larger sample of events from which we can hone our expectations for future gravitational wave sources.

JCAP03(2026)081